Comparative study of the chemical composition and anti-proliferative activities of the aerial parts and roots of *Apium graveolens* L. (celery) and their biogenic nanoparticles

Shereen S. T. Ahmed [a,‡], John Refaat Fahim [a,*‡], Khayrya A. Youssif [b], Mohamed N. Amin [c], Hossam M. H. Abdel-Aziz [d], Ibrahim A. Khadra [e], Mostafa E. Rateb [f], Usama Ramadan Abdelmohsen [a,g], Ashraf Nageeb Elsayed Hamed [a,*]

[a] Department of Pharmacognosy, Faculty of Pharmacy, Minia University, 61519 Minia, Egypt.

[b] Department of Pharmacognosy, Faculty of Pharmacy, Modern University for Technology and Information, Cairo, Egypt.

[c] Department of Biochemistry, Faculty of Pharmacy, Mansoura University, 35516 Mansoura, Egypt.

[d] Department of Pharmaceutical Medicinal Chemistry, Faculty of Pharmacy, South Valley University, Qena, Egypt.

[e] Strathclyde Institute of Pharmacy and Biomedical Sciences, University of Strathclyde, Glasgow G4 0RE, UK.

[f] School of Computing, Engineering & Physical Sciences, University of the West of Scotland, Paisley PA1 2BE, UK.

[g] Department of Pharmacognosy, Faculty of Pharmacy, Deraya University, 61111 New Minia, Egypt.

[‡] Authors have equally contributed to this work.

*** Corresponding Authors:**

Ashraf Nageeb Elsayed Hamed (ashrafnag@mu.edu.eg)

John Refaat Fahim (john.michael@mu.edu.eg)

Abstract

Apiaceae plants are multipurpose folk remedies and bioactive foods that show a remarkable ability to biosynthesize a large number of secondary metabolites with antitumor and chemopreventive potential. Among the various members of the Apiaceae, celery (*Apium graveolens* L.) has long been used as a popular edible and medicinal plant owing to its plentiful health benefits and nutraceutical properties; however, the anticancer potential of this important species has been seldom studied, mostly focusing on its seeds. Therefore, this work was designed to delve into the chemical composition and anti-proliferative potential of the total ethanolic extracts of the aerial parts (TEEAGA) and roots (TEEAGR) of *A. graveolens* var. dulce (Mill.) Pers. as well as their green synthesized silver nanoparticles (AgNPs). In general, both TEEAGA and TEEAGR exhibited moderate to potent inhibitory activities against human liver (HepG-2), colon (Caco-2), and breast (MCF-7) cancer cell lines, with interesting IC_{50} profiles [(41.37 ± 0.12, 27.65 ± 0.27, and 9.48 ± 0.04 µg/mL) and (11.58 ± 0.02, 7.13 ± 0.03, and 6.58 ± 0.02 µg/mL), respectively] as compared with doxorubicin, while more pronounced anti-proliferative effects were observed for their biogenic AgNPs, which showed IC_{50} values ranging between 25.41 ± 0.16 and 1.37 ± 0.03 µg/mL. Moreover, HPLC–HESI–HRMS-based metabolomics analysis of both extracts showed the presence of a varied group of secondary metabolites, including flavonoids, phenylpropanoids, phthalides, coumarins, and sesquiterpenes that further displayed moderate to promising binding affinities to the active site of cyclin G-associated kinase (GAK), particularly graveobioside A, graveobioside B, and celeroside C, suggesting their possible contribution as GAK modulators to the anti-proliferative potential of celery. These findings can help broaden future research on the utilization of different parts of celery and their NPs as functional foods and medicines in cancer chemoprevention and therapy.

Keywords: Anti-proliferative activity; *Apium graveolens* (celery); Biogenic nanoparticles; Chemoprevention; Functional foods; Metabolomics analysis; Nutraceuticals.

1. Introduction

Cancer has become one of the top health challenges of our current world. Recent epidemiological and clinical reports have linked the development of several malignancies, e.g. prostate, breast, lung, and colon cancers with nutrition, defining such pathologies as diet-associated tumors (Deng et al., 2017). Besides genetic influences, both sedentary lifestyles and modern diet have significantly contributed to the increasing incidence and mortality rates of different cancers (Anand et al., 2008). These intricate factors along with the adverse effects and limited efficacy of the currently available chemotherapeutic agents have called attention to the concept of chemoprevention through the use of herbal phytochemicals and nutraceuticals to prevent, delay or reverse carcinogenesis (Salimi et al., 2013). Nutraceuticals include varied groups of secondary metabolites derived from dietary and medicinal plants, and have attracted an increasing interest in recent years owing to their protective and therapeutic potential against many degenerative and chronic conditions, e.g. obesity, cardiovascular system disorders, diabetes, Alzheimer's disease, and cancer. The antioxidant and anti-inflammatory aptitudes of these phytochemicals also afford an additional benefit of enhancing overall health (Prakash et al., 2013).

In view of the growing global demand to explore the chemopreventive role of bioactive foods and natural plant constituents, several studies have substantiated the potential of Apiaceae plants to reduce the risk of multiple cancers and to hamper their progression; a fact that also accounts for their common use as folk medicines, functional foods, as well as food aids and additives (Aćimović, 2017; Aćimović et al., 2018). Among the various plants of Apiaceae, celery (*Apium graveolens* L.) has long been consumed as a medicinal food in several forms, either for its characteristic flavor, health promoting effects or medicinal value (Ingallina et al., 2020). Fresh leaf celery, turnip-rooted celery (celeriac), and celery seeds are commonly used in flavoring and garnishing purposes as well as for the preparation of a range of food items, such as salads, salad dressings, soups, stews, sauces, vegetable juices, biscuits, and pickled vegetables (Aćimović, 2017; Aćimović and Milić, 2017). In herbal medicine, *A. graveolens* is employed

as a diuretic, antispasmodic, anti-parasitic, antihypertensive, anti-arthritic, and anti-rheumatic agent. It also shows helpful sedating effects in nervousness, hysteria, and insomnia (Asif et al., 2011; Fazal and Singla, 2012; Khairullah et al., 2021). As one of the most important functional species in the Apiaceae, different extracts of *A. graveolens* have been reported to exhibit many nutraceutical properties encompassing hypolipidemic, anti-hyperglycemic, anti-platelet aggregation, antimicrobial, laxative, spasmolytic, gastroprotective, hepatoprotective, cardioprotective, antioxidant, cytotoxic, and anti-inflammatory effects (Aćimović, 2017; Khairullah et al., 2021; Sowbhagya, 2014). This meritorious spectrum of health benefits of *A. graveolens* is mainly ascribed to the presence of several classes of chemical metabolites, including flavonoids, phenolic acids, coumarins, phenols, tannins, isobenzofuranoids (phthalides), terpenoids, fatty acids, organic acids, polyalcohols, amino acids, and polysaccharides that have been primarily described from the leaves, petioles, and seeds of the plant (Aćimović, 2017; Al-Asmari et al., 2017; Ingallina et al., 2020). In contrast, little attention has been paid to *A. graveolens* roots where some polyacetylenes and phenolic derivatives have been only reported so far (Al-Asmari et al., 2017; Zidorn et al., 2005). Interestingly, most of the aforementioned groups of metabolites, such as flavonoids, phthalides, coumarins, polyphenols, terpenoids, and polyacetylenes, have been reported to possess wide-ranging anticancer and chemopreventive properties, and thus the consumption of celery was assumed to provide protection against some cancers (Atta, 1998; Aćimović et al., 2018; Ingallina et al., 2020; Khairullah et al., 2021; Köken et al., 2016). Yet, despite the notable biological profile of celery plants, their anti-proliferative potential has been limitedly studied, mostly focusing on the seeds (Al-Jumaily, 2010; Subhadradevi and Kalathil, 2011); therefore, the current study aims to assess and compare the *in vitro* anti-proliferative activities of the total ethanolic extracts of the aerial parts (TEEAGA) and roots (TEEAGR) of *A. graveolens* var. *dulce* (Mill.) Pers. against a panel of human cancer cells, supported with both high-performance liquid chromatography heated electrospray ionization high-resolution mass spectrometry (HPLC–HESI–HRMS)-based metabolomics and molecular docking studies in order to explore different metabolites that might contribute to their anti-proliferative

potential. Additionally, in light of the growing research on the possible role of nutraceutical nanoparticles (NPs) in chemoprevention, the anti-proliferative effects of the green synthesized silver nanoparticles (AgNPs) using TEEAGA and TEEAGR were addressed herein for the first time.

2. Materials and methods

2.1. Chemicals and reagents

Dimethyl sulfoxide (DMSO), ethanol (95%), and sodium hydroxide (NaOH) were bought from El-Nasr Company for Pharmaceuticals and Chemicals, Egypt. Silver nitrate ($AgNO_3$; purity ≥ 99.5 %) was purchased from Sigma-Aldrich, Germany, while acetonitrile (HPLC grade) was obtained from SDFCL sd fine-Chem Limited, Mumbai, India.

2.2. Plant material

Apium graveolens L. var. *dulce* (Mill.) Pers. was collected from the farm of Ornamental, Aromatic, and Medicinal Plants, Faculty of Agriculture, Minia University, Minia, Egypt in April 2018 during the first year of cultivation. These plants were cultivated in wet clay soil with good drainage under low humidity and full sun conditions. The plant material was verified by Prof. Mahmoud A. Hassan, Department of Horticulture, Faculty of Agriculture, Minia University. A voucher specimen (Mn-Ph-Cog-040) was deposited in the herbarium of Pharmacognosy Department, Faculty of Pharmacy, Minia University, Egypt.

2.3. Preparation of extracts

The collected plant material was left for complete drying in the shade at 24–26 ºC and then the roots were detached from the aerial parts. The air-dried, coarsely powdered aerial parts (700 g) and roots (400 g) of *A. graveolens* were separately macerated with 95% ethanol. The alcoholic solutions were then concentrated under vacuum till dryness to afford viscous brown extracts [TEEAGA (32.0 g; yield: 4.57%) and TEEAGR (22.0 g; yield: 5.50%), respectively].

2.4. Metabolomics analysis

Chemical profiling of TEEAGA and TEEAGR was performed by high-performance liquid chromatography heated electrospray ionization high-resolution mass spectrometry (HPLC–HESI–HRMS) technique according to the method described by Mahmoud et al. 2019 and Hamed et al. 2021 using a Dionex UItiMate 3000 HPLC coupled with a Q Exactive™ Hybrid Quadrupole-Orbitrap™ mass spectrometer. Briefly, 10 µL of each sample (1 mg/mL in methanol) were injected into a Phenomenex Kinetex column (2.6 µm XB-C18 150 × 4.6 mm) kept at 30 °C and connected with a guard column. A combination of LC-MS grade water (A) and acetonitrile (B); each containing 0.1% formic acid was used as the mobile phase. Gradient elution was applied at a flow rate of 500 µL/min, beginning with 5% to 20% B within 2 min, 20% to 98% B within 18 min, 98% B for further 5 min, and finally 98% to 5% B within 2 min. Positive and negative ionization modes were used for HESI–HRMS analysis applying the following conditions: capillary temperature (320 °C), sheath gas (57.50), sweep gas (3.25), auxiliary gas (16.25), spray voltage (+3.5 kV or –2.7 kV), probe heater (462.50 °C), S-Lens RF (50), resolution (70.000), maximum IT 100 ms, AGC target (1e6), microscans (1), and a scan range of 150−1500 *m/z*. Differential analysis of mass data was done through MZmine 2.12 and the detected constituents were annotated by comparison with METLIN and the Dictionary of Natural Products (DNP) databases (Abdelhafez et al., 2018, 2020a; Ahmed et al., 2021; Hamed et al., 2021; Zahran et al., 2020).

2.5. Green synthesis and characterization of silver nanoparticles (AgNPs)

A part of the obtained TEEAGA (10 mg) and TEEAGR (25 mg) were separately dissolved in 1 mL DMSO and mixed with 1 mL of 0.001 M $AgNO_3$ and 0.5 mL of 1 N NaOH, then heated for 10 min with stirring at 60 °C. Subsequently, 0.1 mL of each of TEEAGA and TEEAGR was added to 8 and 4.5 mL of 0.001 M $AgNO_3$, respectively, and the final solutions were incubated for 24 h in a dark place at room temperature and checked for any color change, then kept for further 24 h for stabilization. The synthesis of AgNPs was confirmed by measuring the UV–Vis spectrum of the reaction mixtures at 200–600 nm

using a double beam V-630 spectrophotometer (Jasco, Japan), whereas their morphology and size were evaluated by a Transmission Electron Microscope (TEM; Jeol model JEM-1010, USA). Fourier-Transform Infrared Spectroscopy (FT-IR) analysis was also carried out by an FT-IR-8400S spectrophotometer (IR Prestige-21, IR Affinity-1, Shimadzu, Japan) to detect various biomolecules involved in the formation and stabilization of the AgNPs (Abdelhafez et al., 2020b; Ahmed et al., 2021).

2.6. Anti-proliferative activity

The anti-proliferative effects of both TEEAGA and TEEAGR as well as their biosynthesized AgNPs (within 72 h after synthesis) were tested and compared against HepG-2 (hepatocellular carcinoma), Caco-2 (colon carcinoma), and MCF-7 (breast cancer) cell lines obtained from the American Type Culture Collection (Manassas, VA, USA) using the MTT assay (Hamed et al., 2021; Mosmann 1983; Samy et al., 2016). Cells were initially cultured at 37 °C and 5% CO_2 in DMEM high glucose (Invitrogen/Life Technologies, USA) supplemented with 10% FBS (Hyclone, USA), 10 µg/mL of insulin (Sigma-Aldrich, Germany), and 1% penicillin-streptomycin, and then transferred to 96-well plates at a density of 2.2×10^4 cell/cm^2. After overnight incubation, the tested samples were dissolved in DMSO and added to the cultured cells at different concentrations (20, 30, 40, 50, and 60 µg/mL); the viability of cells was then examined by the MTT assay on the next day. In short, the cultured cells were treated with 0.5 mg/mL MTT reagent (150 µL/well) and kept at 37 °C for 3 h. The formed crystals were dissolved by re-incubation with 150 µL DMSO/well for 1h. A microplate reader (Model 550, Bio-Rad, USA) was used to measure the absorbance of each plate at 570 nm. The viability baseline was established using DMSO and the dose-response curve was finally prepared to get the IC_{50} values. Doxorubicin (D1515, Sigma-Aldrich, Germany) was used as a standard. In the same way, AgNPs were added to cells at final concentrations equivalent to those used in the case of celery extracts, while the viability baseline was adjusted using the nano-preparation vehicle without extracts.

2.7. Molecular Docking

Molecular docking simulation was performed to predict and evaluate the binding abilities of the characterized metabolites with the target enzyme cyclin G-associated kinase (GAK). The targeted compounds were presented in a 2D model using the CHEMDRAW software and copied into the MOE interface (version 2019.0101) where the energies of the proposed structures were minimized to attain the most stable conformers that were kept into a database for docking studies. The X-ray crystallographic structure of GAK in complex with gefitinib (PDB Id: 5Y80) was acquired from the protein data bank (https://www.rcsb.org/structure/5Y80), then validated and prepared for docking analysis (RMSD= 1.8 Å). Docking simulations were achieved by the MOE dock tool using Triangle Matcher as a placement scheme, rigid receptor as a refinement scheme, London ΔG as a scoring function, in addition to GBVI/WSAdG as a refinement score. The active site was selected where the original ligand gefitinib occur and docking was performed in the presence of gefitinib through overlaying.

2.8. Statistical analysis

Data were expressed as mean ± standard error of mean. One-way analysis of variance (ANOVA) followed by Dunnett's test was used. Statistical analysis was carried out by GraphPad Prism software (Version 5.01, San Diego, CA, USA). Results were described as significant at $p < 0.05$.

3. Results and discussion

3.1. Metabolomics analysis

HPLC–HESI–HRMS analysis of TEEAGA and TEEAGR showed a large degree of similarity between the metabolic patterns of both extracts and resulted in the annotation of an assortment of chemically diverse metabolites, e.g. phenylpropanoids, flavonoids, phthalides, coumarins, furanocoumarins, and sesquiterpenes (Table 1; Fig. 1; supplementary material Fig. S1 and S2). Through the comparison with the DNP and METLIN databases, the mass ion peak at *m/z* 359.136 for the suggested molecular formula

198 $C_{16}H_{24}O_9$ was annotated as the phenylpropanoids, junipediol A 4-*O*-glucoside **(1a)** and/or junipediol A 8-
199 *O*-glucoside **(1b)**. Both of these structural isomers were previously described among the chemical
200 constituents of *A. graveolens* seeds (Kitajima et al., 2003; Simaratanamongkol et al., 2014), while this is
201 the first report for their identification from the aerial parts and roots of celery. Likewise, two flavonoidal
202 biosides, namely luteolin 7-*O*-apiofuranosyl-(1→2)-glucopyranoside (graveobioside A; **2**) and its 3'-
203 methyl ether (graveobioside B; **3**) were identified from the observed peaks at *m/z* 579.142 and 593.149,
204 together with their corresponding molecular formulas $C_{26}H_{28}O_{15}$ and $C_{27}H_{30}O_{15}$, respectively. Both
205 flavones were characterized in this work from the aerial parts of *A. graveolens* in agreement with Sastri
206 1956, Liu et al. 2017, and Awad et al. 2019 who reported their bioaccumulation by celery leaves and
207 seeds, while only graveobioside B **(3)** was detected herein in the roots (Table 1).

208 In the same context, phthalides have been widely found as typical secondary metabolites of Apiaceae
209 plants, including those in the genus *Apium* (Ingallina et al., 2016; Grube et al., 2019). In this vein, a
210 dihydrophthalide with the molecular formula $C_{13}H_{16}O_2$ was characterized as isovalidene-3a,4-
211 dihydrophthalide **(4)** based on the mass ion peak at *m/z* 205.123. This compound was earlier reported
212 among the constituents contributing to the aroma and flavor of *A. graveolens* leaves and stalks (Gold and
213 Wilson, 1963; Kurobayashi et al., 2006). Further two isomeric hydrophthalides were also identified as
214 senkyunolide J **(5a)** and/or senkyunolide N **(5b)** in harmony with the observed peak at *m/z* 225.112 and
215 the predicted chemical formula $C_{12}H_{18}O_4$. Both molecules were obtained before from *A. graveolens* seeds,
216 showing good inhibitory potential against topoisomerase I and II (Momin and Nair, 2002). Another
217 hydrophthalide with the molecular formula $C_{12}H_{20}O_2$ was characterized as 3-butylhexahydrophthalide **(6)**
218 in line with the mass ion peak at *m/z* 197.154; this molecule was also formerly described from *A.*
219 *graveolens* seeds (Barschat et al., 1997). Moreover, in accordance with the reported literature (Al-Asmari
220 et al., 2017), the current metabolomics study of *A. graveolens* showed the presence of a number of
221 coumarins, represented by compounds **7–10**. Of these, the mass ion peaks at *m/z* 405.129, 263.094, and
222 263.093, corresponding to the chemical formulas $C_{20}H_{22}O_9$, $C_{15}H_{18}O_4$, and $C_{14}H_{14}O_5$, were described as

apiumetin-*O*-glucoside **(7)**, 2-(1,2-dihydroxy-1-methylethyl)-2,3-dihydro-7*H*-furo[3,2g][1]benzopyran-7-one **(8)**, and celereoin **(9)**, respectively. Another related molecule was also characterized as the prenylated coumarin, osthenol **(10)** on account of the mass ion peak at *m/z* 229.086 and the molecular formula $C_{14}H_{14}O_3$. So far, all of the aforementioned coumarin derivatives have been identified from celery seeds only (Garg et al., 1981; Maruyama et al., 2009).

Beyond the above-mentioned groups, the mass ion peak at *m/z* 417.247, consistent with the suggested molecular formula $C_{21}H_{36}O_8$, was annotated as celeroside D **(11a)**, celeroside C **(11b)**, and/or celeroside B **(11c)**; each of these glucosylated eudesmane-type sesquiterpenoids was formerly identified from celery seeds (Kitajima et al., 2003). Noteworthy, all the identified constituents are firstly reported herein from *A. graveolens* roots.

3.2. Green synthesis and characterization of AgNPs

Recent developments in nanoparticles' (NPs) research have resulted in enormous applications in food sciences, medicine, agriculture, and other related fields. Among different forms of NPs, metallic NPs, e.g. gold and silver NPs, have been proven to display unique physical and chemical attributes owing to their submicron sizes (1–100 nm), leading to enhanced pharmacological and therapeutic potential (Abdelhafez et al., 2020, 2021; Hembram et al., 2018). In this respect, plant-mediated synthesis of AgNPs is gaining prominence because of its cost-effectiveness and eco-friendliness, in addition to the promising biomedical applications and noteworthy properties of the produced AgNPs, e.g. chemical stability, biocompatibility, catalytic activity, and biological spectrum which includes anti-inflammatory, antioxidant, antidiabetic, hepatoprotective, and antimicrobial effects (Hembram et al., 2018; Rao et al., 2016). Such plant-based AgNPs have been also widely incorporated in cancer research thanks to their privileged antitumor potential (Alsalhi et al., 2016; Hembram et al., 2018; Rao et al., 2016). Currently, the use of culinary and medicinal herbs' metabolites as chemopreventive and anticancer nutraceuticals is being limited by many stability and bioavailability issues, while loading of these chemicals into NPs has been proven to boost

their physicochemical and biological behavior, which ultimately enriches their role in combating and treating cancer (Huang et al., 2010; Li et al., 2015). Prompted by this, we embarked herein on the green synthesis of AgNPs using *A. graveolens* extracts to study their possible impact on the anti-proliferative potential of this medicinal species.

3.2.1. Color change and TEM characterization of AgNPs

The biogenic preparation of TEEAGA- and TEEAGR-based AgNPs was initially observed by the change of the colorless reaction mixture to a colloidal brown color as the reaction continued (supplementary material Fig. S3) due to the surface plasmon resonance, indicating the successful formation of their corresponding AgNPs (Abdelhafez et al., 2020, 2021; Ahmed et al., 2021; Haggag et al., 2019), while their TEM analysis revealed the formation of spherical particles with mean size ranges of 14.10–25.85 and 15.48–29.12 nm, respectively (Fig. 2).

3.2.2. UV–Vis characterization of AgNPs

In agreement with the literature, the UV–Vis spectra of the reaction mixtures of TEEAGA- and TEEAGR-based AgNPs displayed characteristic absorption maxima at 426 and 425 nm, respectively (Fig. 3), confirming the formation of their respective AgNPs (Abdelhafez et al., 2020, 2021; Ahmed et al., 2021; Haggag et al., 2019). An increment in the absorption intensities was also noticed on increasing the added volumes of $AgNO_3$, which is attributed to the change in the particle size of the formed AgNPs (Tripathy et al., 2010).

3.2.3. FT-IR characterization of AgNPs

Medicinal and food plants contain a variety of phytochemicals that can enhance the reduction of Ag^+ ions to Ag^0 followed by capping, leading eventually to the formation of stable colloidal NPs. Such is the case with celery extracts where the availability of structurally diverse metabolites assisted Ag^+ reduction and allowed the effective synthesis of biogenic AgNPs. Therefore, FT-IR analysis was employed to

evaluate the surface chemistry of the resulting NPs, e.g. chemical bonds and functional atoms, in order to unveil different biomolecules involved in their formation and stabilization (Ahmed et al., 2021; Hembram et al., 2018; Youssif et al., 2019). The obtained FT-IR spectra exhibited a number of peaks in relation to multiple chemical functionalities (Fig. 4 and 5), including those at 3428.81, 2928.38, 2642, 1925.57, 1638.23, 1381.75, 1116.68, 1036.55, 835.99, 772.351, 684.606, 625.788 and 400.70 cm^{-1} (for AgNPs of TEEAGA) as well as at 3752.8, 3429.78, 2925.48, 2555.22, 1929.43, 1627.63, 1383.68, 1026.91, 834.062, and 697.141 cm^{-1} (for AgNPs of TEEAGR), which is in agreement with the reported literature data (Ahmed et al., 2021; Abdelhafez et al., 2020, 2021; Haggag et al., 2019; Youssif et al., 2019). Among the aforementioned FT-IR peaks, the absorbance bands at 3755–3550 cm^{-1} were indicative of the stretching of free O-H groups in alcohols, while those ranging between 3500 and 3200 cm^{-1} were consistent with O-H stretching in alcohols and phenolic compounds with strong hydrogen bonds as well as the stretching of N-H groups of amines (Abdelhafez et al., 2020; Ahmed et al., 2021; Shameli et al., 2012). Furthermore, the observed FT-IR peaks at 3100–2500 cm^{-1} included C-H stretching in alkanes, alkenes, and aldehydes in addition to O-H stretching of carboxylic acids, whereas those at 2140–1900 cm^{-1} indicated the stretching of C≡C in alkynes and C=C=C in allenes. Likewise, the absorbance bands at 1800–1560 cm^{-1} involved the bending of N-H groups in amines and C=C stretching in alkenes, together with the C=O stretching in a variety of carbonyl compounds, e.g. ketones, aldehydes, carboxylic acids, lactones, and esters. The observed peaks in the range of 1400–1300 cm^{-1} were also consistent with the bending of C-H in alkanes and aldehydes and that of O-H in phenols, alcohols, and carboxylic acids (Haggag et al., 2019; Youssif et al., 2019). Finally, the FT-IR peaks appearing at 1200–1000 cm^{-1} corresponded to C-N stretching in amines and C-O stretching in alcohols and aliphatic ethers, whereas those in the range of 1000–550 cm^{-1} were assignable to C-Cl stretching, C=C bending in alkenes, and C-H bending in aromatic compounds (Haggag et al., 2019). The above-mentioned peaks are attributed to the richness of celery extracts in several chemical principles with varied functional groups, such as flavonoids, coumarins, chromones, isobenzofurans, phthalides, polyphenols, terpenoids, glycosides,

proteins, and polysaccharides, which collectively contribute to the capping and stability of the formed NPs, preventing their agglomeration (Abdelhafez et al., 2020, 2021; Ahmed et al., 2021; Hembram et al., 2018; Youssif et al., 2019).

3.3. Anti-proliferative activity

Prior research has indicated the good inhibitory potential of celery against a variety of cancerous cells, with most studies being focused on the seeds. In this respect, the cytotoxic activity of the essential oil of *A. graveolens* var. *filicinum* Crovetto seeds was reported to be attributed to its content of hydrocarbons, among which the three major components, myrcene, 1,3,8-menthatriene, and limonene displayed potent *in vitro* activities against A-549 (lung carcinoma), HT-29 (colon adenocarcinoma), and MCF-7 cell lines (ED_{50} < 10.2 µg/mL) (Saleh et al., 1998). In a similar fashion, the *n*-hexane extract of *A. graveolens* seeds was shown to exert higher *in vitro* inhibitory effects on the rhabdomyosarcoma (RD) cell line compared with its aqueous and ethanolic counterparts, particularly at 200 µg/mL (Al-Jumaily, 2010). The methanolic seed extract of *A. graveolens* was also found to inhibit the proliferation of DLA (Dalton's lymphoma ascites) and L929 (mouse lung fibroblast) cancer cells *in vitro* in a concentration-dependent manner, showing IC_{50} values of 29.79 and 3.85 µg/mL, respectively (Subhadradevi and Kalathil, 2011). In another related work, the ethanolic extract of *A. graveolens* affected the viability of human prostatic carcinoma cells (LNCaP) in both a time- and dose-dependent manner through the induction of apoptosis. Treatment of LNCaP cells with *A. graveolens* extract has also resulted in downregulation of vascular endothelial growth factor (VEGF), which is a key mediator of angiogenesis (Köken et al., 2016). More recently, the total extracts of the leaves and petioles of celery exhibited moderate inhibitory effects (about 33% and 39%, respectively) against *tert*-butyl-hydroperoxide (tBOOH)-induced mutagenicity in the absence of S9, whereas in the presence of S9, the petiole extract showed higher anti-mutagenic potential than that of the blade leaves (about 45% and 32% inhibition was observed at 100 µg/mL, respectively).

Such effects of celery extracts were assumed to be due to their antioxidant activities or other desmutagenic mechanisms (Ingallina et al., 2016). Similarly, the essential oil of celery seeds was reported to prevent CCl_4-induced genotoxicity possibly due to its antioxidant components, e.g. phenolic acids and limonene (Sobti et al., 1991). In the same vein, the cytotoxicity of four polyacetylenes, namely panaxydiol, falcarinol, falcarindiol, and 8-*O*-methylfalcarindiol, obtained from the dichloromethane extract of root celery was described. Of these, falcarinol displayed the highest inhibitory activity, especially against acute lymphoblastic leukemia (CEM-C7H2) cells (IC_{50}= 3.5 µmol/L) (Zidorn et al., 2005).

In view of the aforementioned data, the anti-proliferative activities of TEEAGA and TEEAGR were examined herein for the first time in comparison with doxorubicin as a positive control. As illustrated in Table 2, both extracts inhibited the growth of HepG-2, Caco-2, and MCF-7 tumor cells, with IC_{50} values ranging between 41.37 ± 0.12 and 6.58 ± 0.02 µg/mL. The obtained results also indicated the higher anti-proliferative potential of TEEAGR against the studied cell lines compared with TEEAGA, with the utmost activity of both extracts was recorded against MCF-7 cells (IC_{50}= 6.58 ± 0.02 and 9.48 ± 0.04 µg/mL, respectively); however, their inhibitory effects were lower than doxorubicin in terms of IC_{50} values (Table 2). In light of the US NCI guidelines, these results interestingly uncover the potent (IC_{50} < 20 µg/mL) to moderate (IC_{50}= 21–50 µg/mL) anti-proliferative potential of both celery extracts against the abovementioned cell lines (Boik, 2001; US NCI guidelines), suggesting the broad anticancer spectrum of this important medicinal plant and its potential as a chemopreventive functional food.

Among the various phytoconstituents identified so far from celery, phthalides have been shown to possess a protective role against cancer, exemplified by sedanolide and 3-*n*-butylphthalide that exhibited the ability to stimulate the detoxification enzyme glutathione-*S*-transferase in tumor tissues (Khairullah et al., 2021). Flavonoids and their glycosylated derivatives, such as those of apigenin, luteolin, and kaempferol, have been also reported as common phenolics in different varieties of celery (Mencherini et

al., 2007; Liu et al., 2017; Yao et al., 2010). The capacity of these flavonoids to combat several types of cancer through multiple modes of action has been described, including among others, pancreatic, ovarian, breast, colon, thyroid, leukemia, lung, liver, and prostate cancers (Gates et al., 2009; Hui et al., 2013; Lim et al., 2012; Shukla and Gupta, 2010). Another class of metabolites, namely coumarins, has been also shown to contribute to the protective potential of celery against cell mutations by fighting free radicals (Khairullah et al., 2021). Based on the current investigation of our samples and according to the literature (Csupor-Löffler et al., 2009; Di Sotto et al., 2018; Iranshahi et al., 2018; Kan et al., 2008; Kawaii et al., 2001; Liu et al., 2017), the contribution of different phytochemicals, including flavonoids, coumarins, terpenoids, and phthalides to the anti-proliferative potential of celery can be assumed. Moreover, the individual composition of each of these chemical classes in the roots and aerial parts of celery along with their possible synergistic interactions might underlie the different anti-proliferative potencies of TEEAGA and TEEAGR, which could represent a future research theme in order to correlate such biological effects to specific chemical principles.

On the other hand, a compelling body of evidence has revealed the capacity of nano-sized preparations to refine the compatibility and effectiveness of natural products against cancer, with those packaged as NPs were reported to show higher bioefficacy, more targeted actions, fewer side effects, and lower overall costs than many of the available anticancer drugs (Abdelhafez et al., 2021; Huang et al., 2010; Li et al., 2015; Rao et al., 2016). Therefore, some phytochemicals of nutraceutical value have been loaded as NPs to be used in nano-chemoprevention and nano-chemotherapy, e.g. curcumin, lycopene, lutein, quercetin, and green tea polyphenols (Li et al., 2015; Yadav et al., 2020). Likewise, many studies have substantiated the nutraceutical and therapeutic properties of various nano-preparations of Apiaceae plants, including celery (Alsalhi et al., 2016, 2020; Hembram et al., 2018). In this regard, the anti-osteoarthritis, anti-nociceptive, and antihypertensive potential of celery nanoemulsions were formerly reported (Atta, 1998; Sowbhagya, 2014), while those prepared using celery oil were shown to exert strong antibacterial actions

against *Staphylococcus aureus* and to counteract the growth of oral squamous cell carcinoma (SAS cell line) *in vitro*, with an IC_{50} value of 1.4 µL/mL (Nirmala et al., 2020). The biogenic AgNPs containing celery leaf extract was also proven to have noteworthy fungicidal potential against the two pathogenic species, *Aspergillus niger* and *A. wentii* (Roy et al., 2015). From this standpoint, it was of special interest to explore the anti-proliferative potential of the AgNPs synthesized from the aerial parts and roots of *A. graveolens*. In the main, the AgNPs of both TEEAGA and TEEAGR exhibited more potent inhibitory effects against the studied tumor cells in comparison with the corresponding celery extracts as inferred from their remarkably lower IC_{50} profiles (Table 2), highlighting the possible exceptional role of biogenic AgNPs in enhancing the antitumor properties of celery. Generally, the cytotoxic effect of AgNPs of TEEAGR against the tested cell lines was superior to that exerted by their TEEAGA-based counterparts. Such difference in the potency between TEEAGA- and TEEAGR-based NPs might be underlain by a number of factors that are known to affect the cytotoxicity of AgNPs, including the composition, shape, size, surface charge, and capping biomolecules, among others (Kajani et al., 2014). More interestingly, the inhibitory activities of AgNPs of TEEAGR against HepG-2 cells were largely comparable to doxorubicin (IC_{50}= 1.37 ± 0.02 vs. 1.32 ± 0.06, respectively), whereas their cytotoxic potential against Caco-2 cells was greater than that of doxorubicin (IC_{50}= 1.37 ± 0.03 vs. 2.12 ± 0.04, respectively) (Table 2). These findings evidently tie well with previous studies wherein a vast array of plant-based AgNPs, encompassing those biosynthesized from Apiaceae plants, have been proven to exhibit enhanced antitumor potential, mostly on account of their superior physicochemical and surface properties, large surface to volume ratio, phytochemical loading aptitude, and targeted cellular interactions (Ahmed et al., 2021; Alsalhi et al., 2016; Hembram et al., 2018; Yadav et al., 2020). Moreover, according to the literature, the anticancer effects of AgNPs have been proposed to be triggered by inducing oxidative stress and DNA damage, suppressing ATP synthesis, regulating signaling pathways, counteracting cell cycle and proliferation, and promoting apoptotic events (Rao et al., 2016; Xu et al., 2020).

3.4. Molecular Docking

The inhibition of protein kinases has emerged in recent decades as a crucial strategy for cancer prevention and management owing to their key roles in intracellular signaling which controls cell proliferation, differentiation, and survival (Ohbayashi et al., 2018). Accumulated data have therefore highlighted the potential of numerous plant extracts and metabolites, e.g. alkaloids, phenolics, flavonoids, and terpenoids, to modulate or inhibit different kinases, offering a cornucopia of anticancer drug candidates (Gill et al., 2020; Hou and Kumamoto, 2010). To date, compounds with anti-protein kinase activities have shown efficacy against many cancers, exemplified by the clinically approved epidermal growth factor receptor (EGFR) inhibitor, gefitinib, which is commonly used for the treatment of non-small cell lung cancer (Ohbayashi et al., 2018), but was also found to be effective against liver, breast, and colorectal cancers (Geng et al., 2015; Ponz-Sarvisé et al., 2007; Schiffer et al., 2005). Gefitinib not only interrupts signaling in target cells via EGFR, but also displays high affinity for other protein kinases, e.g. cyclin G-associated kinase (GAK); a kinase that acts as an important EGFR regulator and contributes to receptor signaling and other cellular functions (Ohbayashi et al., 2018; Susa et al., 2010). Geftinib was also shown to exhibit similar binding modes to the common ATP site in both EGFR and GAK, which proposes similar mechanisms of inhibition (Ohbayashi et al., 2018). Recently, GAK has been proven as a potential target for chemoprevention and cancer treatment due to its implication in human malignancy as a master regulator of tumor proliferation and metastasis (Ohbayashi et al., 2018; Susa et al., 2010). Hence, in the present study, molecular docking simulation was employed to seek the possible interactions of metabolites **(1–11)** with GAK using gefitinib as a reference ligand. As depicted in Table 3, most of the docked compounds formed considerably stable complexes within the catalytic domain of GAK, showing moderate to favorable binding scores in the range of –4.90 to –7.93 kcal/mol as compared to gefitinib (–7.84 kcal/mol). These bindings were brought about by the interaction with a variety of amino acid residues, of which Cys126 and Leu46 were equally involved in the interactions shown by many of the docked metabolites, e.g. **2, 3, 6–8, 11a,** and **11b**, as well as gefitinib (Table 3). Among the docked

compounds, the glycosylated derivative of luteolin, graveobioside B **(3)** displayed the highest binding affinity to GAK through a number of interactions with the key amino acids Leu46, Cys126, and Gln129, which was even better than gefitinib in terms of its lower energy score (–7.93 kcal/mol), followed by its demethylated derivative, graveobioside A **(2)** (–7.67 kcal/mol) and the sesquiterpenoid glycoside, celeroside C **(11b)** (–7.24 kcal/mol); both of them had comparable docking scores to gefitinib (–7.84 kcal/mol) (Table 3; Fig. 6 and 7). These results are broadly in line with the previous reports wherein flavonoids have been shown to exert varied chemopreventive properties by binding to some kinases, affecting their phosphorylation state and regulating several signaling pathways involved in carcinogenesis (Hou and Kumamoto, 2010). In this vein, luteolin and its derivatives have been reported as interesting molecules against different human malignancies via inhibition of tumor proliferation, driving out carcinogenic stimuli, stimulation of cell cycle arrest, and induction of apoptosis through multiple signaling pathways (Imran et al., 2019).

Additionally, compounds **1a, 1b, 7,** and **11a** showed as good binding aptitudes as the co-crystallized ligand, gefitinib, with docking scores ranging from –6 to –7 kcal/mol, while **4, 5a, 5b, 8–10,** and **11c** displayed moderate affinities (–5 to –6 kcal/mol) (Table 3). In contrast, 3-butylhexahydrophthalide **(6)** exhibited the lowest binding strength (–4.90 kcal/mol) among all the studied phytocompounds. Taken together, these findings propose the contribution of the characterized metabolites, as possible modulators of GAK, to the observed anti-proliferative activities of celery extracts against HepG-2, Caco-2, and MCF-7 cells. The receptor-ligand interactions formed by these molecules, particularly **2**, **3**, and **11b**, might also afford better insights to design natural therapeutic agents that overcome the side effects of gefitinib.

4. Conclusion

The current work described the anti-proliferative activities of the aerial parts and roots of *A. graveolens* against liver, colon, and breast tumor cells that were shown to be underlain by a diversity of metabolites, e.g. phenylpropanoids, flavonoids, phthalides, coumarins, and sesquiterpenes, as identified by LC–MS-

based metabolomics. Our results also provided evidence for the promising role of nanotechnological approaches, such as the preparation of biogenic NPs, in enhancing the anticancer and functional properties of celery. Moreover, molecular docking analysis of the characterized metabolites suggested their contribution to the anti-proliferative potential of celery extracts as possible inhibitors of GAK, especially graveobiosides A **(2)** and B **(3)** and celeroside C **(11b)**, which revealed prominent interaction aptitudes with GAK. These data highlight the relevance of different parts of celery and their biogenic NPs for the development of anticancer functional foods and drugs, and could provide the basis for future *in vivo* investigations on the anticancer effects of this valued medicinal plant and its secondary metabolites.

Declaration of competing interest

The authors declare no conflict of interest.

Funding

This research did not receive any specific grant from funding agencies in the public, commercial, or not-for-profit sectors.

References

Abdelhafez, O.H., Fawzy, M.A., Fahim, J.R., Desoukey, S.Y., Krischke, M., Mueller, M.J., Abdelmohsen, U.R., 2018. Hepatoprotective potential of *Malvaviscus arboreus* against carbon tetrachloride-induced liver injury in rats. PloS One 13, e0202362.

Abdelhafez, O.H., Othman, E.M., Fahim, J.R., Desoukey, S.Y., Pimentel-Elardo, S.M., Nodwell, J.R., Schirmeister, T., Tawfike, A., Abdelmohsen, U.R., 2020a. Metabolomics analysis and biological investigation of three Malvaceae plants. Phytochem. Anal. 31, 204–214.

Abdelhafez, O.H., Ali, T., Fahim, J.R., Desoukey, S.Y., Ahmed, S., Behery, F.A., Kamel, M.S., Gulder, T., Abdelmohsen, U.R., 2020b. Anti-inflammatory potential of green synthesized silver nanoparticles of the soft coral *Nephthea* sp. supported by metabolomics analysis and docking studies. Int. J. Nanomed. 15, 5345–5360.

514 Abdelhafez, O.H., Fahim, J.R., El Masri, R.R., Salem, M.A., Desoukey, S.Y., Ahmed, S., Kamel, M.S.,
515 Pimentel-Elardo, S.M., Nodwell, J.R., Abdelmohsen, U.R., 2021. Chemical and biological studies on
516 the soft coral *Nephthea* sp. RSC Adv. 11, 23654-23663.
517 Aćimović, M.G., 2017. Nutraceutical potential of Apiaceae. In: Mérillon JM, Ramawat K (eds) Bioactive
518 molecules in food. Reference Series in Phytochemistry, Springer, Cham.
519 Aćimović, M.G., Rat, M.M., Tesevic, V.V., Dojcinovic, N.S., 2018. Anticancer properties of Apiaceae.
520 Bentham Science, UAE, pp. 236–255.
521 Aćimović, M., Milić, N., 2017. Perspectives of the Apiaceae hepatoprotective effects – a review. Nat.
522 Prod. Commun. 12, 309–317
523 Ahmed, S.S.T., Fahim, J.R., Youssif, K.A., Amin, M.N., Abdel-Aziz, H.M.H, Brachmanne, A.O., Piel, J.,
524 Abdelmohsen, U.R., Hamed, A.N.E., 2021. Cytotoxic potential of *Allium sativum* L. roots and their
525 green synthesized nanoparticles supported with metabolomics and molecular docking analyses. S. Afr.
526 J. Bot. 142, 131–139.
527 Al-Asmari, A.K., Athar, M.T., Kadasah, S.G., 2017. An updated phytopharmacological review on
528 medicinal plant of Arab region: *Apium graveolens* Linn. Pharmacog. Rev. 11, 13–18.
529 Al-Jumaily, R.M.K., 2010. Evaluation of anticancer activities of crude extracts of *Apium graveolens* L.
530 seeds in two cell lines, RD and L20B *in vitro*. Iraqi J. Cancer Med. Genet. 3, 18–23.
531 Alsalhi, M.S., Devanesan, S., Alfuraydi, A.A., Vishnubalaji, R., Munusamy, M.A., Murugan, K.,
532 Nicoletti, M., Benelli, G., 2016. Green synthesis of silver nanoparticles using *Pimpinella*
533 *anisum* seeds: antimicrobial activity and cytotoxicity on human neonatal skin stromal cells and colon
534 cancer cells. Int. J. Nanomed. 11, 4439–4449.
535 Alsalhi, M.S., Devanesan, S., Atif, M., AlQahtani, W.S., Nicoletti, M., Serrone, P.D., 2020. Therapeutic
536 potential assessment of green synthesized zinc oxide nanoparticles derived from fennel seeds extract.
537 Int. J. Nanomed. 15, 8045–8057.
538 Anand, P., Kunnumakkara, A.B., Sundaram, C., Harikumar, K.B., Tharakan, S.T., Lai, O.S., Sung, B.,
539 Aggarwal, B.B., 2008. Cancer is a preventable disease that requires major lifestyle changes. Pharm.
540 Res. 25, 2097–2116.
541 Asif, H.M., Akram, M., Usmanghani, K., Akhtar, N., Shah, P., Uzair, M., Ramzan, M., Shah, S.M.,
542 Rehman, R., 2011. Monograph of *Apium graveolens* Linn. J. Med. Plant. Res. 5, 1494–1496.
543 Atta, A., 1998. Anti-nociceptive and anti-inflammatory effects of some Jordanian medicinal plant
544 extracts. J. Ethnopharmacol. 60, 117–124.

545 Awad, H.A., Awda, J.M., Abd-Alssirag, M., Allaalfalahi, D., 2019. GC-mass analysis of (*Apium*
546 *graveolens*) leaf extracts obtained with aqueous and methanol extraction and study its antimicrobial
547 activity. Asian J. Microbiol. Biotechnol. Environ. Sci., 21, 84–90.
548 Barschat, D., Beck, T., Mosandi, A., 1997. Stereoisomeric flavor compounds. 79. simultaneous enantio-
549 selective analysis of 3-butylphthalide and 3-butylhexahydrophthalide stereoisomers in celery, celeriac,
550 and fennel. J. Agric. Food Chem. 45, 4554–4557.
551 Boik, J. Natural Compounds in Cancer Therapy, Oregon Medical Press, Princeton, Minn, USA, 2001.
552 Csupor-Löffler, B., Hajdú, Z., Zupkó, I., Réthy, B., Falkay, G., Forgo, P., Hohmann, J., 2009.
553 Antiproliferative effect of flavonoids and sesquiterpenoids from Achillea millefolium s.l. on cultured
554 human tumour cell lines. Phytother. Res. 23, 672–676.
555 Deng, F.E., Shivappa, N., Tang, Y., Mann, J.R., Hebert, J.R., 2017. Association between diet-related
556 inflammation, all-cause, all-cancer, and cardiovascular disease mortality, with special focus on
557 prediabetics: findings from NHANES III. Eur. J. Nutr. 56, 1085–1093.
558 Dictionary of Natural Products. http://dnp.chemnetbase.com/faces/chemical/Chemical-Search.xhtml.
559 Accessed on 17 December 2020.
560 Di Sotto, A., Abete, L., Toniolo, C., Mannina, L., Locatelli, M., Giusti, A. M., Nicoletti, M., Vecchiato,
561 M., Di Giacomo, S., 2018. *Capsicum annuum* L. var. Cornetto di Pontecorvo PDO: polyphenolic
562 profile and in vitro biological activities. J. Funct. Foods 40, 679−691.
563 Fazal, S.S., Singla, R.K., 2012. Review on the pharmacognostical and pharmacological characterization
564 of *Apium graveolens* Linn. Indo Glob. J. Pharm. 2, 36–42.
565 Garg, S.K., Sharma, N.D., Gupta, S.R., 1981. A new dihydrofurocoumarin from *Apium graveolens*.
566 Planta Med. 43, 306–308.
567 Gates, M.A., Vitonis, A.F., Tworoger, S.S., Rosner, B., Titus-Ernstoff, L., Hankinson, S.E., Cramer, D.
568 W., 2009. Flavonoid intake and ovarian cancer risk in a population-based case-control study. Int. J.
569 Cancer 124, 1918–1925.
570 Geng, D., Sun, D., Zhang, L., Zhang, W. 2015. The therapy of gefitinib towards breast cancer partially
571 through reversing breast cancer biomarker arginine. Afr. Health Sci. 15, 594–597.
572 Gill, M.S.A., Saleem, H., Ahemad, N., 2020. Plant extracts and their secondary metabolites as modulators
573 of kinases. Curr. Top. Med. Chem. 20, 1093–1104.
574 Gold, H.J., Wilson, C.W., 1963. The volatile flavor substances of celery. J. Food Sci. 28, 484–488.
575 Grube, K., Spiegler, V., Hensel, A., 2019. Antiadhesive phthalides from *Apium graveolens* fruits against
576 uropathogenic *E. coli*. J. Ethnopharmacol. 237, 300–306.

Haggag, E.G., Elshamy, A.M., Rabeh, M.A., Gabr, N.M., Salem, M., Youssif, K.A., Samir, A., Bin Muhsinah, A., Alsayari, A., Abdelmohsen, U.R., 2019. Antiviral potential of green synthesized silver nanoparticles of *Lampranthus coccineus* and *Malephora lutea*. Int. J. Nanomed. 14, 6217–6229.

Hamed, A., Abdelaty, N.A., Attia, E.Z., Amin, M.N., Ali, T., Afifi, A.H., Abdelmohsen, U.R., Desoukey, S.Y., 2021. Antiproliferative potential of *Moluccella laevis* L. aerial parts family Lamiaceae (Labiatae), supported by phytochemical investigation and molecular docking study. Natural Product Research 1–5, In press. https://doi.org/10.1080/14786419.2021.1876046.

Hembram, K.C., Kumar, R., Kandha, L., Parhi, P.K., Kundu, C.N., Bindhani, B.K., 2018. Therapeutic prospective of plant-induced silver nanoparticles: application as antimicrobial and anticancer agent. Artif. Cells Nanomed. Biotechnol. 46(sup3), S38–S51.

Hou, D.X., Kumamoto, T., 2010. Flavonoids as protein kinase inhibitors for cancer chemoprevention: direct binding and molecular modeling. Antioxid. Redox Signal. 13, 691–719.

Huang, Q., Yu, H., Ru, Q., 2010. Bioavailability and delivery of nutraceuticals using nanotechnology. J. Food Sci. 75, R50–57.

Hui, C., Qi, X., Qianyong, Z., Xiaoli, P., Jundong, Z., Mantian, M., 2013. Flavonoids, flavonoid subclasses and breast cancer risk: A meta-analysis of epidemiologic studies. PLoS ONE 8, e54318.

Imran, M., Rauf, A., Abu-Izneid, T., Nadeem, M., Shariati, M.A., Khan, I.A., Imran, A., Orhan, I.E., Rizwan, M., Atif, M., Gondal, T.A., Mubarak, M.S., 2019. Luteolin, a flavonoid, as an anticancer agent: A review. Biomed. Pharmacother. 112, 108612.

Ingallina, C., Capitani, D., Mannina, L., Carradori, S., Locatelli, M., Di Sotto, A., Di, Giacomo. S., Toniolo, C., Pasqua, G., Valletta, A., Simonetti, G., Parroni, A., Beccaccioli, M., Vinci, G., Rapa, M., Giusti, A.M., Fraschetti, C., Filippi, A., Maccelli, A., Crestoni, M.E., Fornarini, S., Sobolev, A.P., 2020. Phytochemical and biological characterization of Italian "sedano bianco di Sperlonga" protected geographical indication celery ecotype: A multimethodological approach. Food Chem. 309, 125649.

Iranshahi, M., Rezaee, R., Najaf Najafi, M., Haghbin, A., Kasaian, J., 2018. Cytotoxic activity of the genus *Ferula* (Apiaceae) and its bioactive constituents. Avicenna J. Phytomed. 8, 296–312.

Kajani, A.A., Bordbar, A.K., Esfahani, S.H., Khosropour, A.R., Razmjou, A., 2014. Green synthesis of anisotropic silver nanoparticles with potent anticancer activity using *Taxus baccata* extract. RSC Adv. 4, 61394–61403.

Kan, W. L., Cho, C. H., Rudd, J. A., Lin, G., 2008. Study of the anti-proliferative effects and synergy of phthalides from Angelica sinensis on colon cancer cells. J. Ethnopharmacol. 120, 36–43.

Kawaii, S., Tomono, Y., Ogawa, K., Sugiura, M., Yano, M., Yoshizawa, Y., 2001. The antiproliferative effect of coumarins on several cancer cell lines. Anticancer Res. 21, 917–923.

610 Khairullah, A.R., Solikhah, T.I., Ansori, A.N.M., Hidayatullah, A.R., Hartadi, E.B., Ramandinianto, S.C.,
611 Fadholly, A., 2021. Review on the pharmacological and health aspects of *Apium graveolens* or celery:
612 An update. Sys. Rev. Pharm. 12, 606–612.

613 Kitajima, J., Ishikawa, T., Satoh, M., 2003. Polar constituents of celery seed. Phytochemistry 64, 1003–
614 1011.
615 Köken, T., Koca, B., Özkurt, M., Erkasap, N., Kuş, G., Karalar, M., 2016. *Apium graveolens* extract
616 inhibits cell proliferation and expression of vascular endothelial growth factor and induces apoptosis in
617 the human prostatic carcinoma cell line LNCaP. J. Med. Food 19, 1166–1171.
618 Kurobayashi, Y., Kouno, E., Fujita, A., Morimitsu, Y., Kubota, K., 2006. Potent odorants characterize the
619 aroma quality of leaves and stalks in raw and boiled celery. Biosci. Biotechnol. Biochem. 70, 958–65.
620 Li, C., Zhang, J., Zu, Y.J., Nie, S.F., Cao, J., Wang, Q., Nie, S.P., Deng, Z.Y., Xie, M.Y., Wang, S. 2015.
621 Biocompatible and biodegradable nanoparticles for enhancement of anti-cancer activities of
622 phytochemicals. Chin. J. Nat. Med. 13, 641–652.
623 Lim, Y.D., Cho, J.H., Kim, J., Nho, C.W., Lee, K.W., Park, J., 2012. Luteolin decreases IGF-II
624 production and downregulates insulin-like growth factor-I receptor signaling in HT-29 human colon
625 cancer cells. BMC Gastroenterol. 12, 9.
626 Liu, G., Zhuang, L., Song, D., Lu, C., Xu, X., 2017. Isolation, purification, and identification of the main
627 phenolic compounds from leaves of celery (*Apium graveolens* L. var. *dulce* Mill. /Pers.). J. Sep. Sci.
628 40, 472–481.
629 Mahmoud, B., Hamed, A.N., Samy, M., Abdelmohsen, U.R., Attia, E., Fawzy, M., Refaey, R.H., Salem,
630 M., Pimentel-Elardo, S., Nodwell, J., Desoukey, S.Y., Kamel, M.R., 2019. Metabolomic profiling and
631 biological investigation of *Tabebuia aurea* (Silva Manso) leaves, family Bignoniaceae. Nat. Prod. Res.
632 1-6. https://doi.org/10.1080/14786419.2019.1698571.
633 Maruyama, T., Abbaskhan, A., Choudhary, M.I., Tsuda, Y., Goda, Y., Farille, M., Reduron, J.P., 2009.
634 Botanical origin of Indian celery seed (fruit). J. Nat. Med. 63, 248–253.
635 Mencherini, T., Cau, A., Bianco, G., Della Loggia, R., Aquino, R. P., Autore, G., 2007. An extract of
636 *Apium graveolens* var. *dulce* leaves: Structure of the major constituent, apiin, and its anti-inflammatory
637 properties. J. Pharm. Pharmacol. 59, 891–897.
638 METLIN. http://metlin.scripps.edu/index.php. Accessed on 15 December 2020.
639 Momin, R.A., Nair, M.G., 2002. Antioxidant, cyclooxygenase and topoisomerase inhibitory compounds
640 from *Apium graveolens* Linn. seeds. Phytomedicine 9, 312–318.

641 Mosmann, T., 1983. Rapid colorimetric assay for cellular growth and survival: application to proliferation
642 and cytotoxicity assays. Journal of Immunological Methods 65, 55–63.
643 Mzmine. http://sourceforge.net/projects/mzmine/. Accessed on 2 November 2020.
644 National Cancer Institute. https://dtp.cancer.gov/databases_tools/docs/compare/compare_methodology
645 .htm. Accessed on 3 October 2021.
646 Nirmala, M.J., Durai, L., Gopakumar, V., Nagarajan, R., 2020. Preparation of celery essential oil-based
647 nanoemulsion by ultrasonication and evaluation of its potential anticancer and antibacterial
648 activity. Int. J. Nanomed. 15, 7651–7666.
649 Ohbayashi, N., Murayama, K., Kato-Murayama, M., Kukimoto-Niino, M., Uejima, T., Matsuda, T.,
650 Ohsawa, N., Yokoyoma, S., Nojima, H., Shirouzu, M.. 2018. Structural basis for the inhibition of
651 cyclin G-associated kinase by gefitinib. ChemistryOpen 7, 721–727.
652 Ponz-Sarvisé, M., Rodríguez, J., Viudez, A., Chopitea, A., Calvo, A., García-Foncillas, J., Gil-Bazo, I.,
653 2007. Epidermal growth factor receptor inhibitors in colorectal cancer treatment: what's new? World
654 J. Gastroenterol. 13, 5877–5887.
655 Prakash, D., Gupta, C., Sharma, G., 2012. Importance of phytochemicals in nutraceuticals. J. Chin. Med.
656 Res. Develop. 1, 70–78.

657 Rao, P. V., Nallappan, D., Madhavi, K., Rahman, S., Wei, L.J., Gan, S.H., 2016. Phytochemicals and
658 biogenic metallic nanoparticles as anticancer agents. Oxid. Med. Cell. Longev. 2016, 3685671.

659 Roy, K., Sarkar, C.K., Ghosh, C.K., 2015. *Apium graveolens* leaf extract-mediated synthesis of silver
660 nanoparticles and its activity on pathogenic fungi. Digest. J. Nanomater. Biostruct. 10, 393–400.
661 Saleh, M.M., Hashem, F.A., Glombitza, K.W., 1998. Cytotoxicity and *in vitro* effects on human cancer
662 cell lines of volatiles of *Apium graveolens* var. *filicinum*. Pharm. Pharmacol. Lett. 8, 97–99.
663 Salimi, A., Seydi, E., Pourahmad, J., 2013. Use of nutraceuticals for prevention and treatment of cancer.
664 Iran. J. Pharm. Sci. 12, 219–220.

665 Samy, M.N., Hamed, A.N.E., Sugimoto, S., Otsuka, H., Kamel, M.S., Matsunami, K., 2016.
666 Officinalioside, a new lignan glucoside from *Borago officinalis*, Nat. Prod. Res. 30, 967–972.
667 Sastri, B.N., 1956. The wealth of India. A dictionary of Indian raw materials and industrial products.
668 Council of Scientific and Industrial Research, New Delhi.
669 Schiffer, E., Housset, C., Cacheux, W., Wendum, D., Desbois-Mouthon, C., Rey, C., Clergue, F., Poupon,
670 R., Barbu, V., Rosmorduc, O., 2005. Gefitinib, an EGFR inhibitor, prevents hepatocellular carcinoma
671 development in the rat liver with cirrhosis. Hepatology 41, 307–314.

672 Shameli, K., Bin Ahmad, M., Jaffar Al-Mulla, E.A., Ibrahim, N.A., Shabanzadeh, P., Rustaiyan, A.,
673 Abdollahi, Y., Bagheri, S., Abdolmohammadi, S., Usman, M.S., Zidan, M., 2012. Green biosynthesis
674 of silver nanoparticles using *Callicarpa maingayi* stem bark extraction. Molecules 17, 8506–8517.
675 Shukla, S., Gupta, S., 2010. Apigenin: A promising molecule for cancer prevention. Pharm. Res. 27, 962–
676 78.
677 Simaratanamongkol, A., Umehara, K., Noguchi, H., Panichayupakaranant, P., 2014. Identification of a
678 new angiotensin-converting enzyme (ACE) inhibitor from Thai edible plants. Food Chem. 165, 92–97.
679 Sobti, R.C., Mittal, O.P., Sachdeva, A., Gill, G.B., 1991. Anticlastogenic effect of essential oil of seeds of
680 *Apium graveolens*. Cytologia 56, 303–308.
681 Sowbhagya, H.B., 2014. Chemistry, technology, and nutraceutical functions of celery (*Apium graveolens*
682 L.): an overview. Crit. Rev. Food Sci. Nutr. 54, 389–398.
683 Subhadradevi, V., Kalathil, K., 2011. Induction of apoptosis and cytotoxic activities of *Apium graveolens*
684 Linn. using *in vitro* models. Middle East J. Sci. Res. 9, 90–94.
685 Susa, M., Choy, E., Liu, X., Schwab, J., Hornicek, F. J., Mankin, H., Duan, Z., 2010. Cyclin G-associated
686 kinase is necessary for osteosarcoma cell proliferation and receptor trafficking. Mol. Cancer Ther. 9,
687 3342–3350.
688 The Protein Data Bank. https://www.rcsb.org/structure/6M8B) (PDB Id: 6M8B). Accessed on 15 March
689 2021.
690 Tripathy, A., Raichur, A.M., Chandrasekaran, N., Prathna, T.C., Mukherjee, A., 2010. Process variables
691 in biomimetic synthesis of silver nanoparticles by aqueous extract of *Azadirachta indica* (Neem)
692 leaves. J. Nanoparticle Res. 12, 237–246.
693 Xu, L., Wang, Y.Y., Huang, J., Chen, C.Y., Wang, Z.X., Xie, H., 2020. Silver nanoparticles: synthesis,
694 medical applications and biosafety. Theranostics 10, 8996–9031.
695 Yadav, N., Parveen, S., Banerjee, M., 2020. Potential of nano-phytochemicals in cervical cancer
696 therapy. Clin. Chim. Acta 505, 60–72.
697 Yao, Y., Sang, W., Zhou, M., Ren, G., 2010. Phenolic composition and antioxidant activities of 11 celery
698 cultivars. J. Food Sci. 75, C9–C13
699 Youssif, K.A., Haggag, E.G., Elshamy, A.M., Rabeh, M.A., Gabr, N.M., Seleem, A., Salem, M.A.,
700 Hussein, A.S., Krischke, M., Mueller, M.J., Abdelmohsen, U.R., 2019. Anti-Alzheimer potential,
701 metabolomic profiling and molecular docking of green synthesized silver nanoparticles
702 of *Lampranthus coccineus* and *Malephora lutea* aqueous extracts. PLoS ONE 14, e0223781.
703 Zahran, E.M., Abdelmohsen, U.R., Ayoub, A.T., Salem, M.A., Khalil, H.E., Desoukey, S.Y., Fouad,
704 M.A., Kamel, M.S., 2020. Metabolic profiling, histopathological anti-ulcer study, molecular docking

and molecular dynamics of ursolic acid isolated from *Ocimum forskolei* Benth. (family Lamiaceae). S. Afr. J. Bot. 131, 311–319.

Zidorn, C., Jöhrer, K., Ganzera, M., Schubert, B., Sigmund, E., Mader, J., Greil, R., Ellmerer, E., Stuppner, H., 2005. Polyacetylenes from the Apiaceae vegetables carrot, celery, fennel, parsley, and parsnip and their cytotoxic activities. J. Agric. Food Chem. 53, 2518–2523.

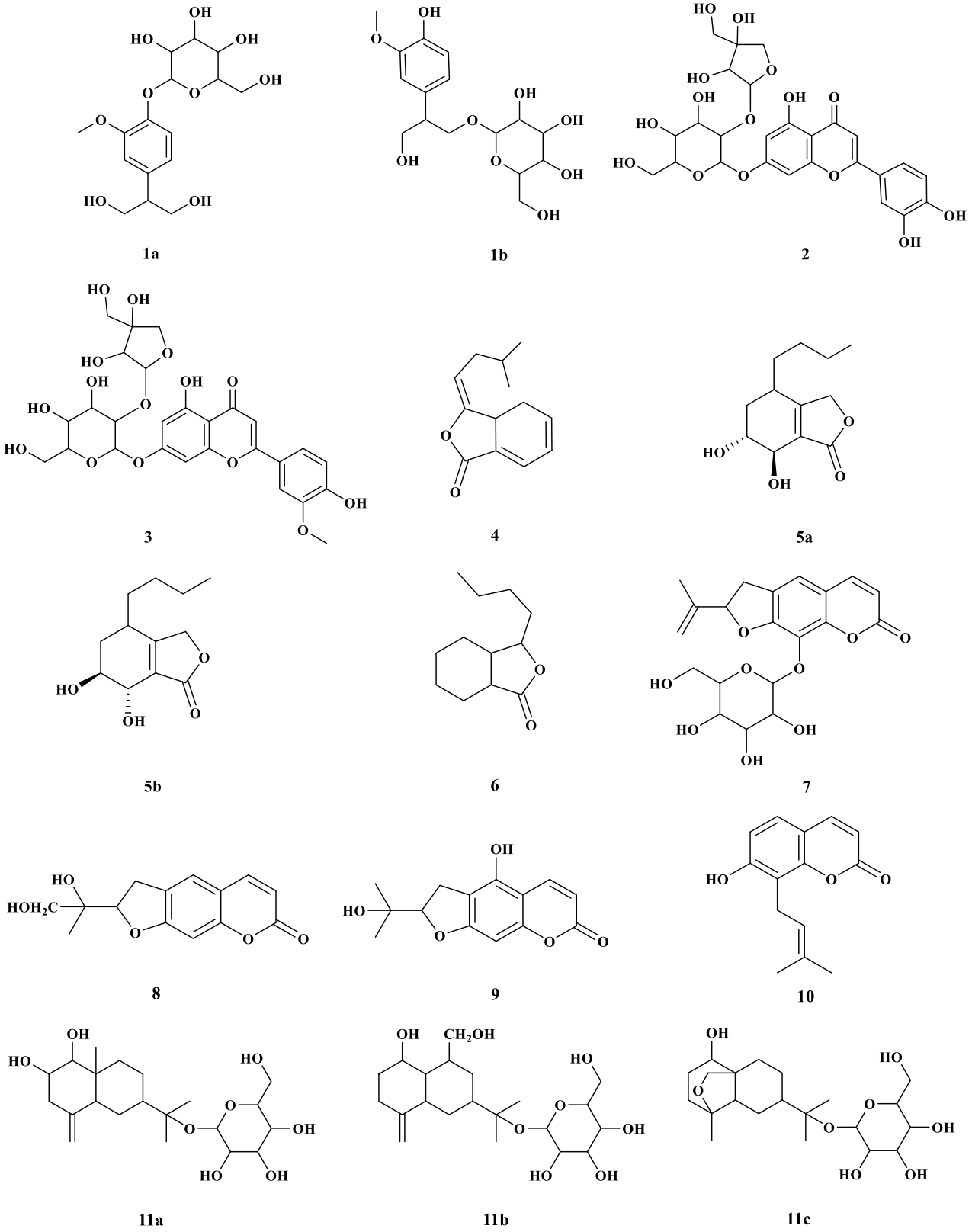

Fig. 1. Chemical structures of the tentatively characterized metabolites from *A. graveolens*.

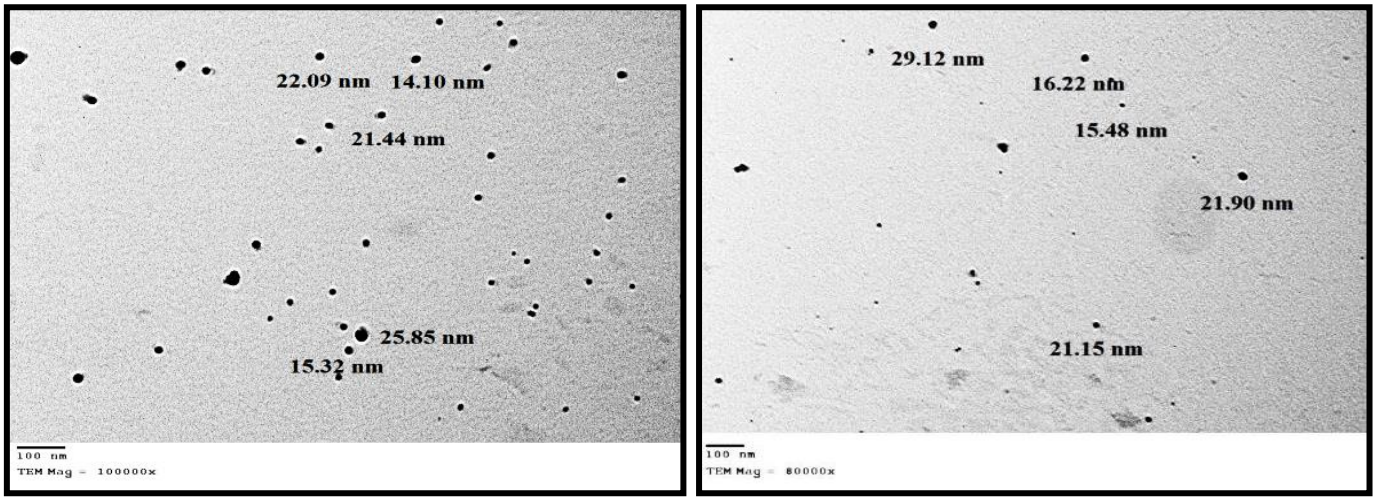

(a) (b)

Fig. 2. TEM photos for the shape and size of AgNPs of TEEAGA (a) and TEEAGR (b).

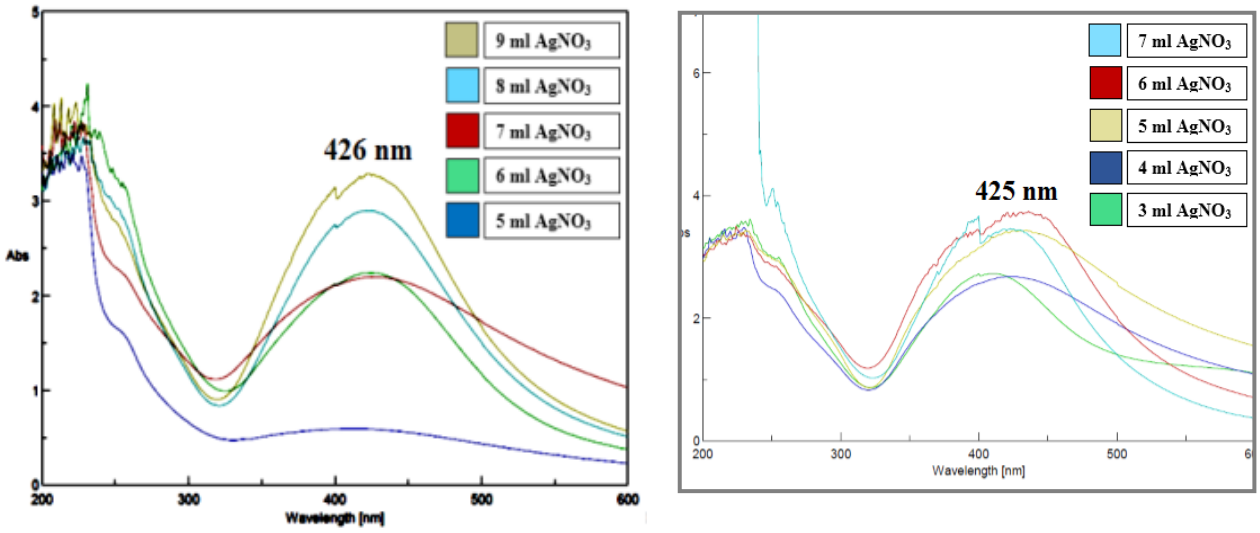

(a) (b)

Fig. 3. UV–Vis spectral analysis and color intensity AgNPs of TEEAGA (a) and TEEAGR (b).

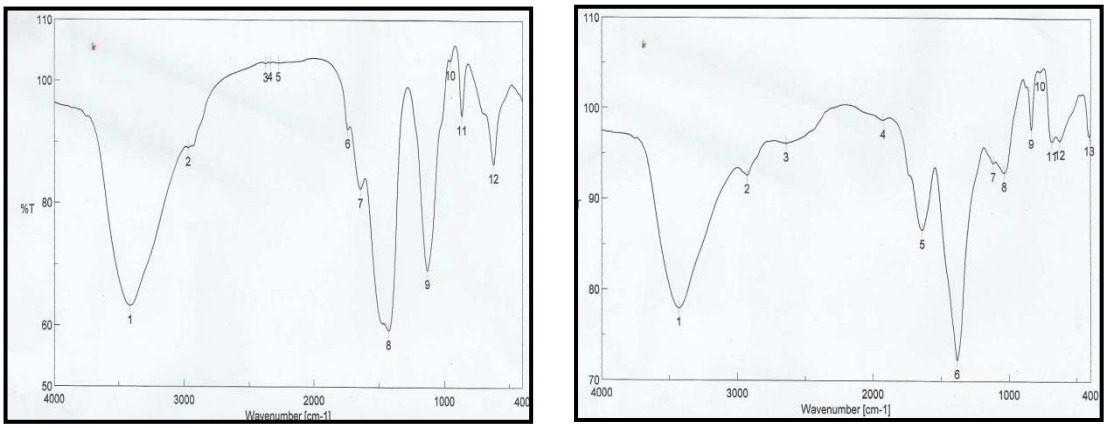

(a) (b)

Fig. 4. FT-IR spectra of TEEAGA (a) and after synthesis of TEEAGA AgNPs (b).

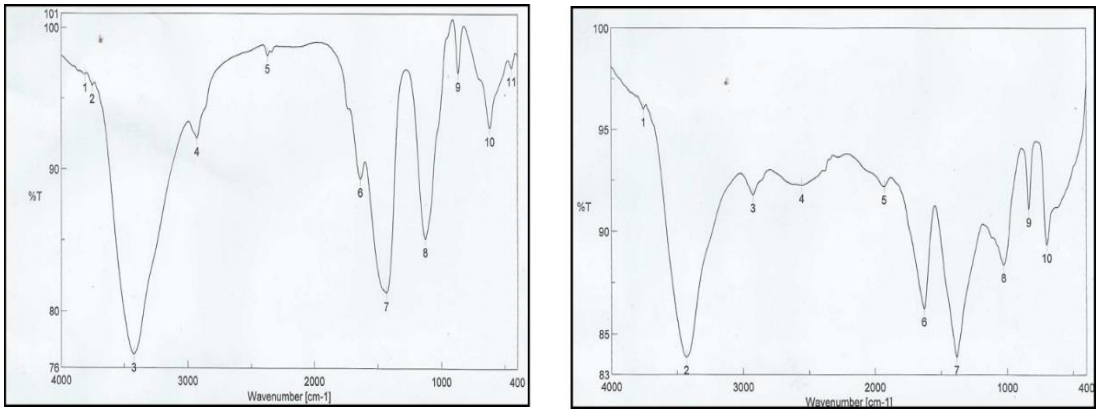

(a) (b)

Fig. 5. FT-IR spectra of TEEAGR (a) and after synthesis of TEEAGR AgNPs (b).

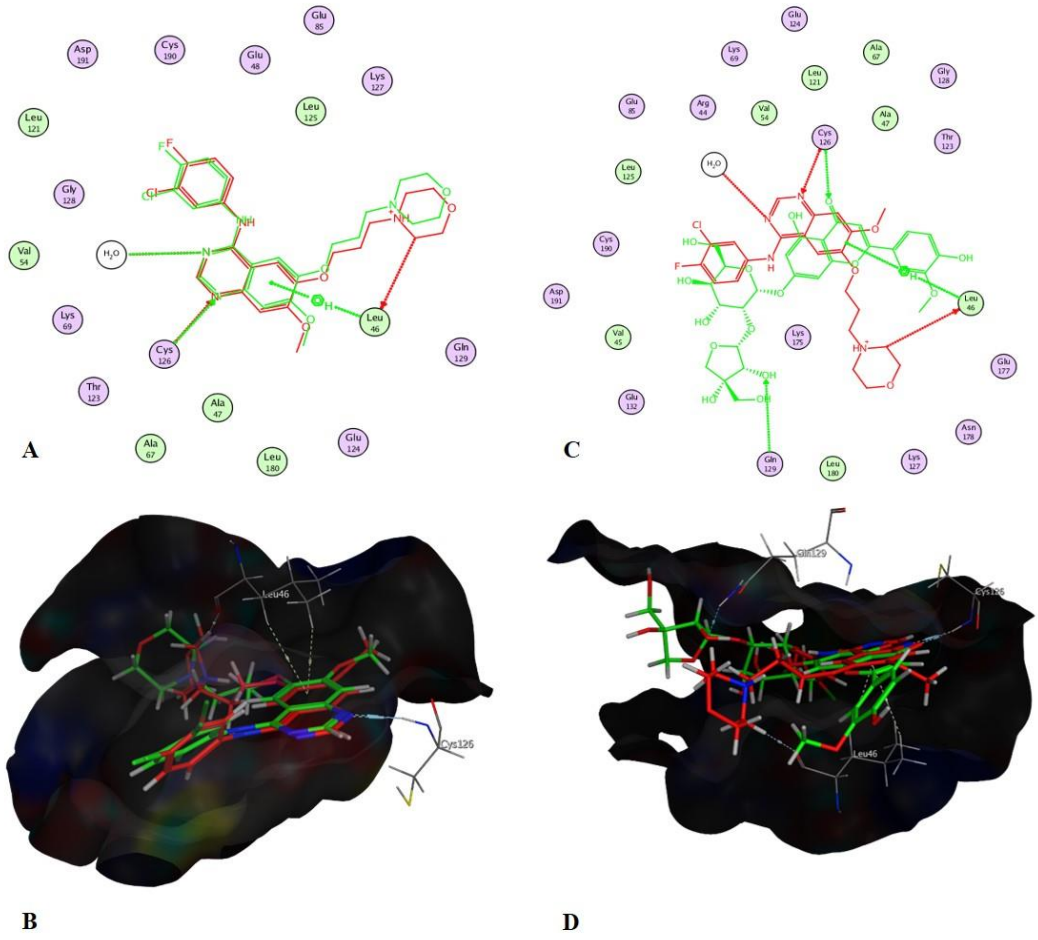

Fig. 6. 2D and 3D illustration of the interactions between the targeted compounds and GAK; (A and B): gefitinib and (C and D): graveobioside B.

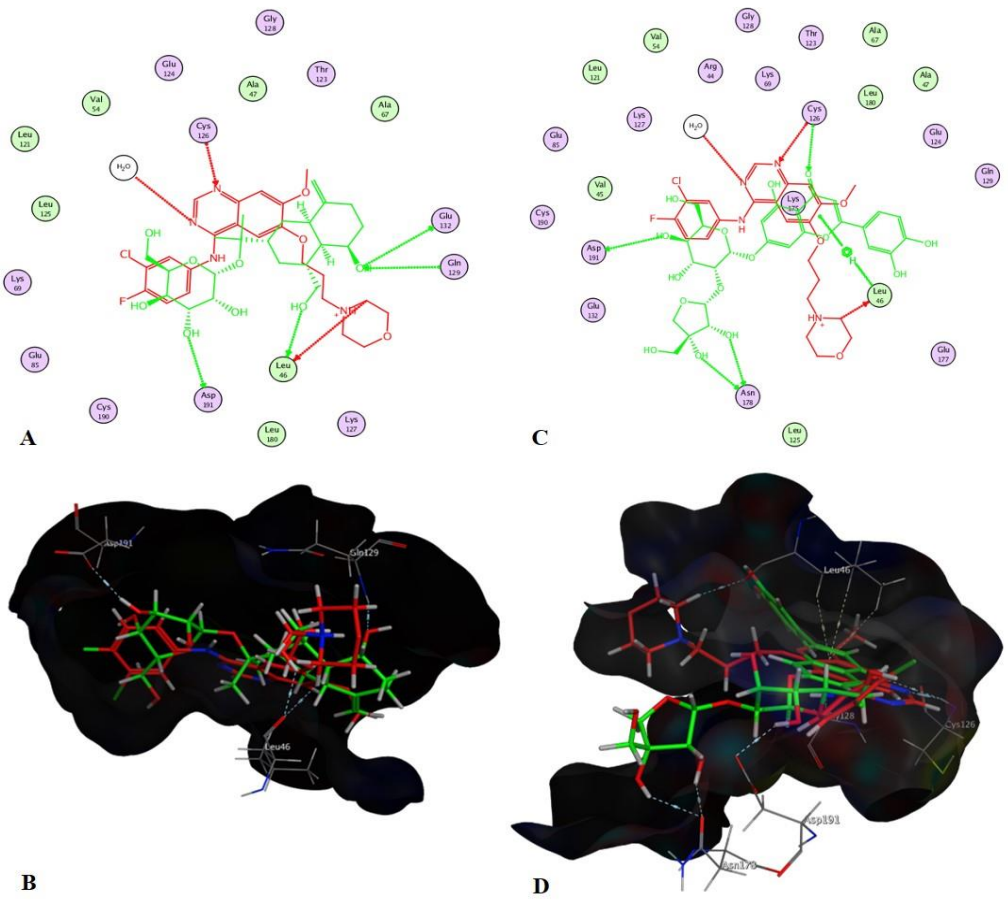

Fig. 7. 2D and 3D illustration of the interactions between the targeted compounds and GAK; (A and B): celeroside C and (C and D): graveobioside A.